A Monte Carlo Study of the DUMAND II Array

A. Okada
Institute for Cosmic Ray Research,
University of Tokyo, Tanashi, Tokyo 188, Japan

Abstract

A simulation of the DUMAND II array as a muon detector is described in detail. The angular resolution for a traversing muon with its incident zenith angle θ larger than 80° is 0.6° ~2.3° expressed in terms of the median of the error distribution, dependening on θ and the energy. The corresponding effective detection area is ~20000 m^2 at θ = 120° where it is nearly maximized.

1. Introduction

The design of the optical sensor array for DUMAND II [1] (Deep Underwater Muon And Neutrino Detector) being proposed has been confirmed by Monte Carlo studies mainly done by V. J. Stenger [2]. Under the requirement that the muon track can be reconstructed with an angular resolution of ~ 1° , parameters such as the distance between optical modules are determined so as to maximize the effective detection area. Here the optical module means an unit of the optical sensor containing a photomultiplier to detect Cherenkov light emitted from charged particles.

Why we have begun Monte Carlo simulations also in Japan is as follows :

- Independent studies are useful to increase the reliability of the design.
- There are several subjects which have not been investigated at all or completely.
- The characteristics of the optical module for which our Japanese group is responsible are related directly to the array design and its capability. We need to quickly know any effect produced, for instance, by changing a part of design of the photomultiplier during the development of the optical module.

Here, as a preliminary step, we present our way of simulation of a muon passing through the array, a method of muon track reconstruction and the resultant angular resolution of the reconstructed track from the simulated event. The

track. On the other hand, we treat an interaction energy loss equal to or larger than 0.1 GeV as a catastrophic one. The integral rate of such catastrophic event per meter along muon path is shown in Fig.1 as a function of the energy loss (i.e. shower energy) with a parameter of muon energy. The Cerenkov light from a catastrophic energy loss is obtained from an analytical solution of Cerenkov light from cascade shower[4]. It has an angular dependence, and the shape of the curve varys also with the distance from the shower. For now we fix the curve simply like that in Fig.2 [5].

The absorption length (λ) of light in the deep ocean is assumed to be 40 m. In a strict sense, however, the whole light in the wavelength band where the bi-alkali photocathode of PMT is sensitive does not decrease just simply like $\exp(-r/\lambda)$, because the absorption length depends much on the wavelength. Here we follow Ref.6 with respect to this problem.

The number of photons reaching the PMT in the OM is assumed to fluctuate with a Poissonian distribution.

Even if a muon track is given, the arrival time of Cerenkov light at an OM is not determined uniquely, but depends on where the light has been emitted from on the muon track. Supposing we can neglect the lateral spread of cascade showers, the earliest light is from the muon itself which is emitted in the direction of 42° off the muon track. Light from showers is generally delayed if the angle from the muon track is different from 42° , the larger the difference of the angle, the more the delay time. It sometimes happens that the OM detects only light from showers and no light from muon itself. This delayed time data causes a somewhat complicated situation in reconstructing the muon track. We will mention this problem again in Section 6.

The background light is mainly due to Cerenkov light from the beta-decay electrons of Potassium (K^{40}) and bioluminescense. Here without distinguishing between them, we assume complete random noise in the PMT output (100 KHz) ascribed to the background light. (Recently, very interesting results about bioluminescence were obtained by the DUMAND collaboration[7),8)]. We will have to take into account those result in the next refined version of the simulation. But according to Ref.8, the bioluminescence takes place mainly in the neighborhood of OM and the correlation between OMs is weak. So the present assumption is useful enough as the first approximation.)

Finally we get a set of data about pulse height and detection time in each OM in an event. In the following Sections, the threshold of pulse height is set at 1/3 of the most probable single photoelectron pulse height. In Fig.6(a) and Fig.7(a), typical simulated muon events are drawn.

effective detection area is discussed at the same time. Those muons which we are most interested in have incident zenith angles larger than 80° and are expected to have been produced in neutrino interactions. The overwhelming majority are the atmospheric muons coming down with small zenith angles. Then, the reconstructed zenith angle of an atmospheric muon could happen to have a very large error and become a background of neutrino events. That problem is also mentioned below.

2. Simulation of traversing muon

The DUMAND II array is composed of 9 'strings' of optical modules tethered from the bottom of the deep ocean. Eight of the strings are set so as to form an octagon with equal sides of 40 m and one is at the center of the octagon. A string has 24 optical modules attached every 10 m. The photomultiplier(PMT) in the optical module has a nearly spherical shape with a diameter of 15 inches and is fixed to look downward. We assume that the time resolution is 3 ns as standard deviation and the detection efficiency η of a photon including the quantum efficiency is 20 % when the photon comes right in front, that is, in parallel with the central axis of the PMT, and it decreases as the angle θ between the photon and the central axis increases ;

$$\eta \sim 0.52 + 0.48 \cos\theta \quad .$$

This assumption comes from an experimental result about the prototype optical modules which actually were used in the deep ocean for tests[3].

The number of photoelectrons detected each time is assumed to fluctuate following a Poisson distribution. Further the data is smeared by the finite resolving power of PMT. We assume that the pulse height distribution for a single photoelectron is approximated by a Gaussian with 100 % resolution. This assumption and that of the time resolution above are moderate and reasonable ones we will be able to achieve without much difficulty.

While traversing the array, muon loses its energy through continuous ionization and electromagnetic and hadronic interactions. A part of the lost energy is emitted in the form of Cerenkov light from the muon itself (~200 photons per cm) and from electrons produced in the interactions and the consequent developments of cascade showers. The OM detects such Cerenkov light. Here, for the convenience of calculation, when the muon energy loss (i.e. transferred energy) in an interaction is smaller than 0.1 GeV, we treat it as a continuous energy loss and add the equivalent energy to the ionization loss. The resultant continuous Cerenkov light from muon is increased a little, which is assumed to be emitted in the direction of Cerenkov angle ~42° from the muon

3. Trigger conditions and the effective trigger area

Here, we follow the trigger condition Stenger makes in his simulation[1], though another way of triggering has been proposed[9].

First, Stenger's condition deals with merely those hit OMs which have at least one adjacent hit OM in the string, where a hit OM means a OM from which a signal comes out in a reasonable time after a muon passes through the array. (Actually, since the time when the muon passes is unknown, a little more complicated definition is needed.) The above condition is taken into account, because an isolated hit OM which has no adjacent hit OM must have a higher probability that the signal is due to the background.

Next, a set of two or three strings must have one of combinations shown in the right table about the minimum numbers of such adjacent OMs in each string. That is the event trigger condition.

patterns
4 - 2 - 2
3 - 3 - 2
5 - 2 - 0
4 - 3 - 0

Table 1

In Fig. 3, the effective trigger areas as a function of muon zenith angle (Fig. 3(a)) and as that of muon energy (Fig. 3(b)) are shown for muon events satisfying the above trigger requirements.

But, even for such muon events, all the muon tracks are not necessarily reconstructed uniquely. It is easily seen that the third and fourth patterns (i.e. the case that only two strings have hit OMs) have at least two solutions for the track, being symmetric to each other with respect to the plane including the two strings. The first and second patterns can also have two solutions if the three strings lie in a straight line. Of course, that sort of event is not useless, but we will eliminate events of the sort beforehand in the following Sections. The effective trigger areas without such events are shown by dot curves in Fig. 3. Further, some of the remaining events fail in the track reconstruction. That is mentioned in Section 5.

Along with the background light, the effective trigger area looks to increase somewhat. In Fig. 3 no background is considered.

In Fig. 4 and Fig. 5, the averaged number of OMs and the averaged number of Strings per triggered event are shown respectively also as a function of muon zenith angle (Fig. 4(a), Fig. 5(a)) and as that of muon energy (Fig. 4(b), Fig. 5(b)).

4. Reconstruction of muon track

We try to reconstruct muon tracks by using simulated data. Parameters to express a straight muon trajectory are determined so that the trajectory best reproduces both the data of detection time and number of photoelectrons at the OMs by assuming that a relativistic muon emits Cerenkov light constantly while traveling along the trajectory.

In order to define a straight line, four parameters are needed. Another one is required for the time, and moreover it is useful to introduce a parameter to stand for the muon energy because the average yield of Cerenkov light depends on the muon energy. Here, the above 6 parameters are determined by the least square method. Namely, the parameters, x, y, l, m, τ and α, are determined so as to minimize the following function ;

$$F = \frac{\sum_{i=1}^{N} (T_i(x,y,l,m) + \tau - t_i)^2}{\sigma_t^2} + \frac{\sum_{i=1}^{N'} (\alpha \cdot H_i(x,y,l,m) - h_i)^2}{\sigma_h^2}$$

Here,

x, y ; Spatial position on a plane where muon track intersects,

l, m ; The corresponding directional cosines of the muon track,

$T_i(x,y,l,m)$, $H_i(x,y,l,m)$; Time and pulse height (in units of photoelectrons) given as a function of the parameters expressing the muon track (x, y, l, m) and the coordinates expressing the location of each OM.

t_i , h_i ; Data of time and pulse height (in photoelectrons) at each OM.

σ_t , σ_h ; Although more examination might be required, here assumed are

$$\sigma_t = 3 \text{ ns}$$
$$\sigma_h = \sqrt{0.158 h_i^2 + 1.58 h_i + 1.58}$$

We have tried a few methods to find a set of values of the parameters which gives the smallest value to the function F. So far, the most satisfactory method from both the viewpoints of reliability and computing time is one going through the following procedure.

(1) A very rough muon trajectory is estimated directly from data by a simple calculation. For the purpose, we have used the weighted mean position of hit OMs in each string and the averaged difference of time between adjacent OMs. Our estimated error is within about 45° for the direction and within 30 m for the spatial position.

(2) Around the roughly estimated trajectory, a four-dimesional grid of ~20° interval regarding the direction and ~15m interval regarding the spatial position is conceived, and the least square method is applied every time starting with the parameters at every crossing on the grid.
(3) The derivative of the function F differentiated by one of the parameters is equal to zero at the minimum of F. Here the derivative is approximated with the first order Taylor's expansion at the above starting point with respect to the 6 parameters. So the best displacements of the parameters from the starting point to minimize F are given as the solutions of 6 one-dimensional simultaneous equations. Then again starting from the obtained values of the parameters, the same procedure is repeated twice.
(4) Among the values of the function F obtained starting from the different crossings on the grid, the smallest value is adopted as the chi-square value, and the acompanying values of parameters are the final ones to express the reconstructed muon track.

The reason why we have to go through such a complicated procedure as the above one is that the function F has many local minima. If there are several minima between adjacent crossings of the grid, we need a much finer grid mesh to reach the true answer. But for a finer grid, for example, with a half interval, the computing time will increase by 16 times. The Facom M780 needs about 1 sec of the CPU time per event to perform the above procedure, whereas the expected muon rate coming in DUMAND is one per 20 sec. We will have enough time to deal further more carefully with neutrino candidates (i.e. events with computed zenith angles greater than 80°).

5. Angular resolution of muon track

As mentioned in Section 3, we exclude isolated hit OMs also in the calculation of reconstruction, because they have higher probability to have received background noise. Here, we call the OM 'isolated OM' when neither its next nor its next but one OMs have no signals in a string.

On the other hand, OMs themselves having no signals can supply us some information. Since it is implausible that an OM close to a muon track has no signal, reconstructed tracks having such non-hit OMs nearby must have been wrongly fitted in the least square method. In the present calculation, the second (pulse height) term in the function F includes the non-hit OMs being within 15 m from the track. Then when $h_i = 0$, the term tends to be large, and F scarcely can be a minimum there.

Extremely large signals from showers or large time deviations, due to backgrounds etc., decrease the quality of reconstruction. We try to eliminate such data from the function F in the procedure of the reconstruction mentioned above.

In Fig.6 and Fig.7, samples of events are shown. A detailed explanation about these Figures is in the Figure Captions. In Fig.6(a) and Fig.7(a), circles indicate pulse heights at corresponding OMs. In Fig.6(b) and Fig.7(b), circles indicate positive or negative deviations of time data from the fitted time. In Fig.7, there is a pair of background hits, which is successfully eliminated in the least square calculation. However, all backgrounds are not always eliminated.

In Fig.8 is an example of the reduced chi-square distribution. The events with the reduced chi-square smaller than 4 are selected and their errors of reconstructed angles are plotted in Fig.9. This angular resolution depends on both the muon zenith angle and the muon energy. In Table 2, medians of the angular errors at different zenith angles and energies, together with the corresponding effective detection areas (m^2), are listed. These effective areas are about 80 % of the selected trigger events in Section 3 (i.e. dotted curves in Fig.3). On the other hand, without the background light, about 90 % turns out to be reconstructed.

Zenith angle / Muon Energy	90°	120°	150°	180°
100 GeV	2.25° (13000)	1.53° (14700)	0.90° (11900)	0.92° (4300)
500 GeV	1.81° (16200)	1.32° (18300)	0.84° (13300)	0.68° (5900)
2500 GeV	1.50° (19700)	1.26° (22400)	0.86° (15600)	0.63° (7100)

Table 2

The statistical errors of values in Table 2 are typically 0.03° and 500 m^2. The averaged effective detection area in the zenith angle region larger than 80° is ~16300 m^2 for the 500 GeV muon events.

6. False neutrino events caused by atmospheric muons

If the zenith angle of a muon is larger than 80° , the muon is thought to be produced through a neutrino interaction. In the region of zenith angles much smaller than 80° , atmospheric muons are dominant. In the case that the error of reconstruction for an atmospheric muon is very large and its reconstructed

zenith angle happens to exceed 80° . the muon is misjudged to originate from a neutrino.

The probability that light from a downgoing muon hit OMs is small compared to those from an upgoing muon, because the PMT faces downward. So the fraction of light from showers and backgrounds is larger for the downgoing atmospheric muon events, which makes the reconstruction more difficult. For instance, as mentioned in Section 2, when an OM detects light only from showers and no light from muon itself, the corresponding time data is often somewhat delayed. The dashed curve in Fig. 10 shows the integral number of such OMs per event as a function of the delayed time.

Among 7003 triggered events of atmospheric muons, there are six events which have a reconstructed zenith angle larger than 80° . We have enough time to check those particular events more carefully. Actually, two events are left still over 80° after re-fitting the six events with three times finer grids. The two corresponds to roughly 10 % of those expected muon events triggered above 80° which originate from atmospheric neutrinos.

The muons in the two events pass near the edge of the array, and at a glance the reconstructed muon track does not look to be the best fitted one. So we can still improve our method of the reconstruction. At the same time, final hand scanning may be useful.

7. Conclusion

The present simulation of muon events and the method of track reconstruction are not the final version, and we will have to continue their improvement. Thus the conclusions here are tentative ones.

1) The angular resolution is dependent on the zenith angle and the energy, and is about 0.6° ~2.3° median error for fitted events (~80 % of the triggered events). Typically, the resolution is 1.3° at 120° zenith angle and 500 GeV of the energy.

2) The effective detection area averaged over the zenith angle larger than 80° is ~16300 m^2 for the fitted 500 GeV muon events. If the events ambiguous about the muon direction are included, the effective detection area would increase by ~20 %.

3) It rarely happens that the reconstructed zenith angle of a downgoing atmospheric muon exceeds 80° . However, the rate is about 10 % of neutrino-induced muon events.

Acknowledgements

The author would like to acknowledge the valuable advices of Prof's. Y.Ohashi, K.Kobayakawa and K.Mitsui. Thanks are particularly due to Prof.J.G.Learned who read the manuscript and made helpful comments.

Though the software programing of the Monte Carlo has been developed independently, Prof.V.J.Stenger's talks and reports have motivated much of the present work.

The facilities of the INS computer center, University of Tokyo, were used for the present calculation.

References

(1) DUMAND II proposal, HDC-2-88 (Hawaii DUMAND Center)

(2) A Monte Carlo study of the DUMAND II array by V.J.Stenger is in Ref.(1).
V.J.Stenger's recent studies are in ;
DIR-2-89 (DUMAND Internal Report) and HDC-1-90 (Hawaii DUMAND Center).

(3) S.Matsuno et al.; Nuc. Inst. & Meth., A276, 359 (1989)
J.Babson et al.; to be published in Phys. Rev. D1

(4) J.Nishimura; 15th Inter. Cosmic Ray Conf., 6, 259 (1977)
A.A.Belyaev, I.P.Ivanenko and V.V.Makarov;
15th Inter. Cosmic Ray Conf., 6, 253 (1977)

(5) A.Roberts; Proc. of the 1978 DUMAND Summer Workshop, 1, 103 (1978)

(6) J.G.Learned; Memo HDC 81-10

(7) T.Aoki et al.; Nuovo Cimento, 9C, 624 (1986)

(8) M.S.Webster et al.; submitted to Nature or Deep-Sea Research

(9) J.G.Learned proposes a trigger method which considers the simplicity of hardware structure for speedy triggering. We will test it elsewhere.

Figure Captions

Fig.1 ; Integral rate of cascade showers per meter along muon path vs. the shower energy. The three curves have different muon energies indicated in the figure.

Fig.2 ; Relative Cerenkov light intensity from a cascade shower as a function of the polar angle.

Fig.3 ; The effective trigger area satisfying the trigger requirements shown in Table 1 (solid curve), and the effective area left after discarding apparently ambiguous events in which the muon track can never be uniquely determined (dot curve).

In Fig.3(a), the horizontal axis indicates the muon zenith angle with a

fixed muon energy of 500 GeV. In Fig.3(b), the horizontal axis indicates the muon energy with a fixed zenith angle of 120° .

Fig.4 ; The averaged number of Optical Modules per triggered event as a function of muon zenith angle with a fixed muon energy of 500 GeV (Fig.4(a)), and as that of muon energy with a fixed zenith angle of 120° (Fig.4(b)).

Fig.5 ; The averaged number of Strings per triggered event as a function of muon zenith angle with a fixed muon energy of 500 GeV (Fig.5(a)), and as that of muon energy with a fixed zenith angle of 120° (Fig.5(b)).

Fig.6 ; An illustrated example of a muon event (E_μ=500 GeV, θ=120°). The DUMAND array is viewed from a position 250 m far from and 250 m above the center of the array. The signs '+' in the Fig.6(a) indicate positions of optical modules. The two arrows indicate incoming and outgoing locations of muon. The head of the incoming arrow and the tail of the outgoing arrow correspond to the incoming and outgoing locations on the imaginary wall of cylinder drawn by dashed curves, respectively. Arrows with solid shaft mean that they are on the top or the front side wall and those with dotted shaft do on the bottom or the rear side wall.

In Fig.6(a), circles on optical modules indicate numbers of photoelectrons detected. The smallest circle corresponds to a single p.e., and the area of each circle is in proportion to the number of p.e.'s.

In Fig.6(b), the arrow indicates the reconstructed muon track. The area of circle is in proportion to the time deviation from the reconstructed track. When the mark '+' is in the circle, the deviation is positive. Without the mark in the circle, the deviation is negative. When a signal data is eliminated during the fitting procedure, the mark 'x' is put down in the circle.

Fig.7 ; An illustrated example of muon event (E_μ=500 GeV, θ=120°) with two background hits. The mark '*' in the Fig.7(a) means hit of background light during the muon traverses the array. When a background data is eliminated successfully in the fitting process, the mark '*' is put down in the Fig.7(b).

Fig.8 ; An example of the reduced chi-square distribution.

Fig.9 ; The error distribution of reconstructed angles for the events with chi-squares smaller than 4 in Fig.8.

Fig.10 ; Integral number of hit Optical Modules per atmospheric muon event vs. the delay time of light originated from showers. The solid curve is for all the OMs having signals from showers and the dashed one is only for those OMs which have no signal directly from muons but from showers.

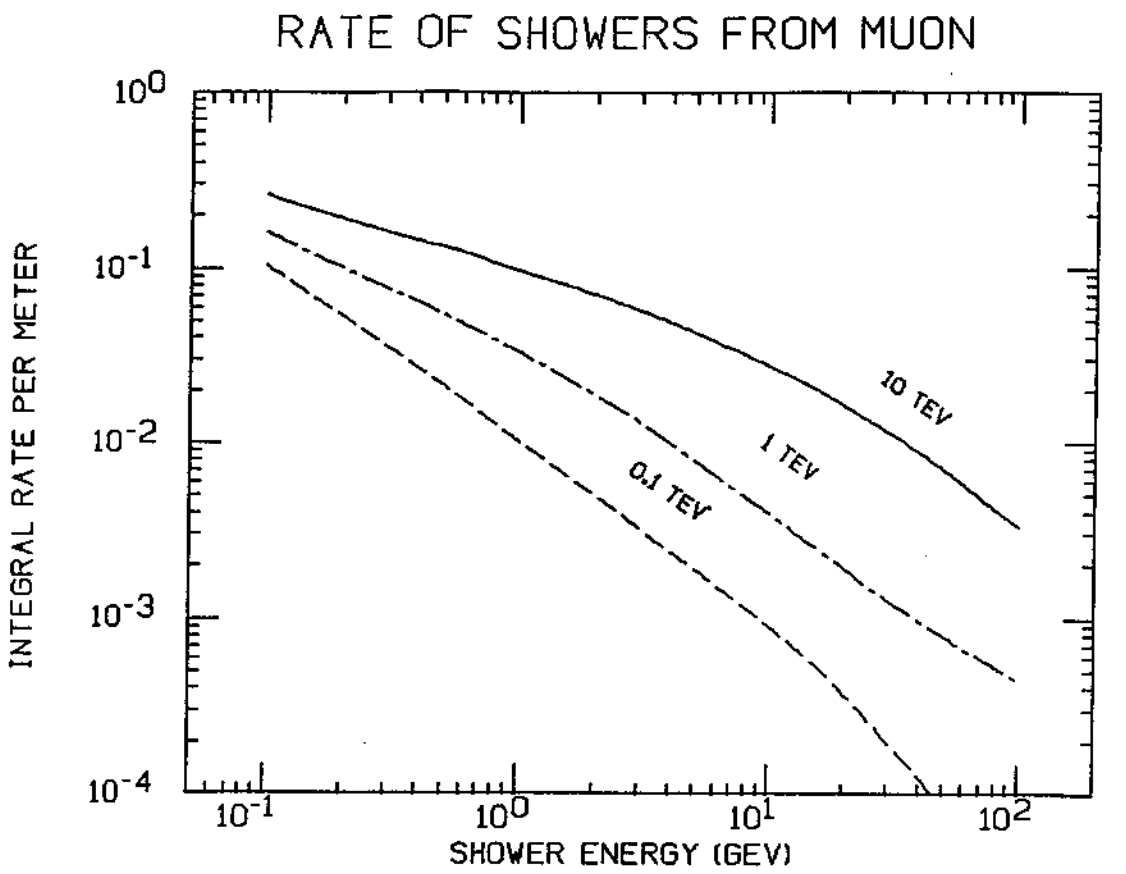
RATE OF SHOWERS FROM MUON
INTEGRAL RATE PER METER
10^0
10^{-1}
10^{-2}
10^{-3}
10^{-4}
10 TEV
1 TEV
0.1 TEV
10^{-1}
10^0
10^1
10^2
SHOWER ENERGY (GEV)

Fig.1

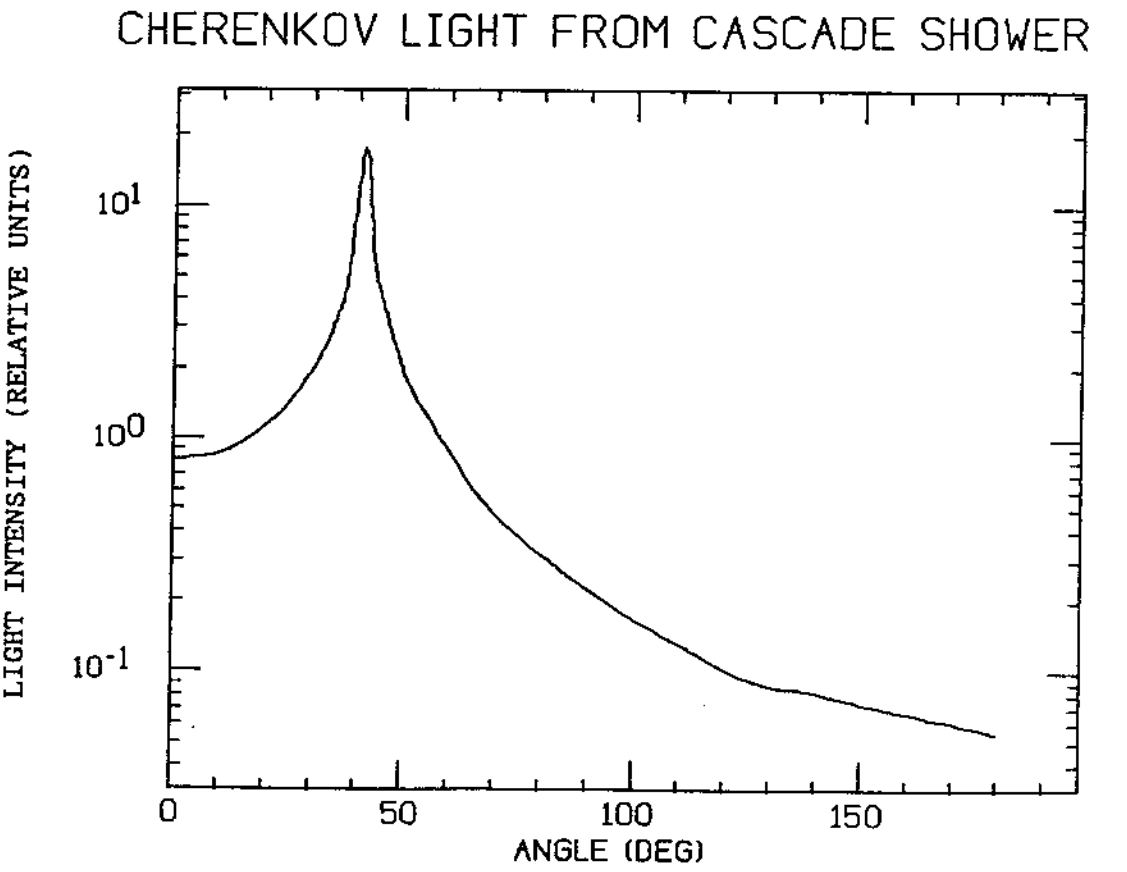
CHERENKOV LIGHT FROM CASCADE SHOWER
LIGHT INTENSITY (RELATIVE UNITS)
10^1
10^0
10^{-1}
0
50
100
150
ANGLE (DEG)

Fig.2

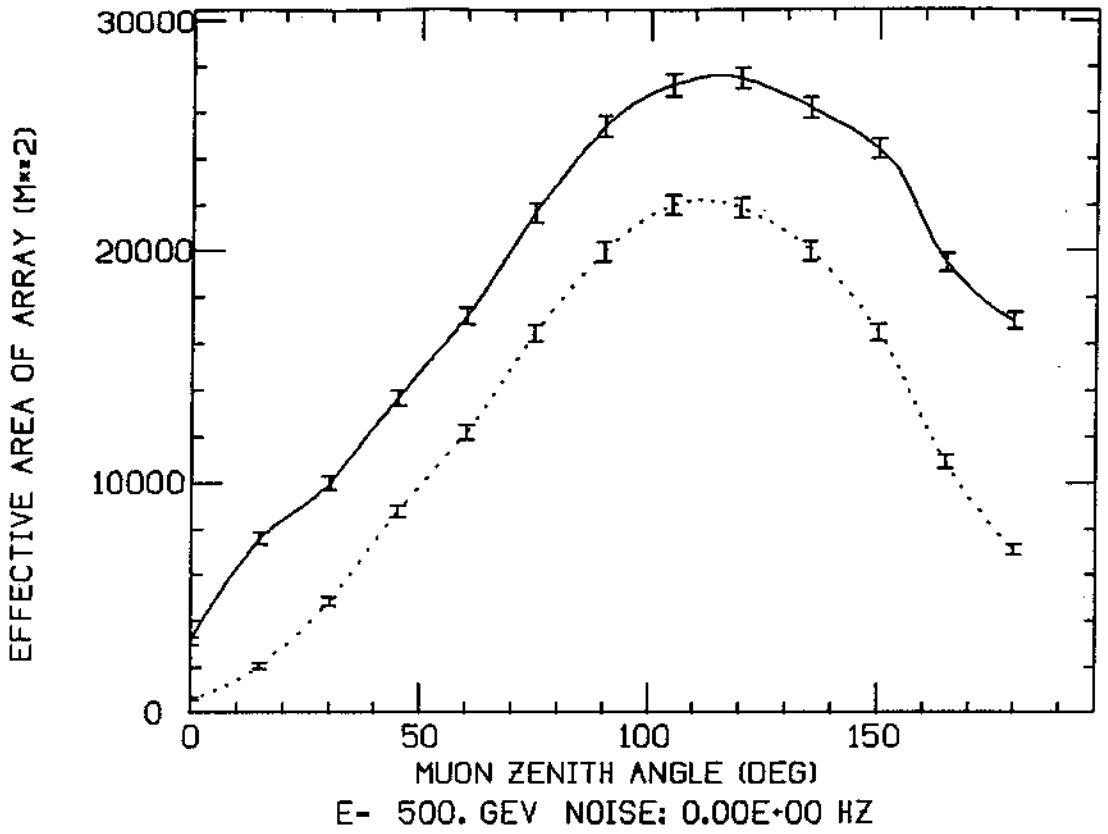
30000
20000
10000
0
EFFECTIVE AREA OF ARRAY (M**2)
0
50
100
150
MUON ZENITH ANGLE (DEG)
E- 500. GEV NOISE: 0.00E+00 HZ

Fig.3(a)

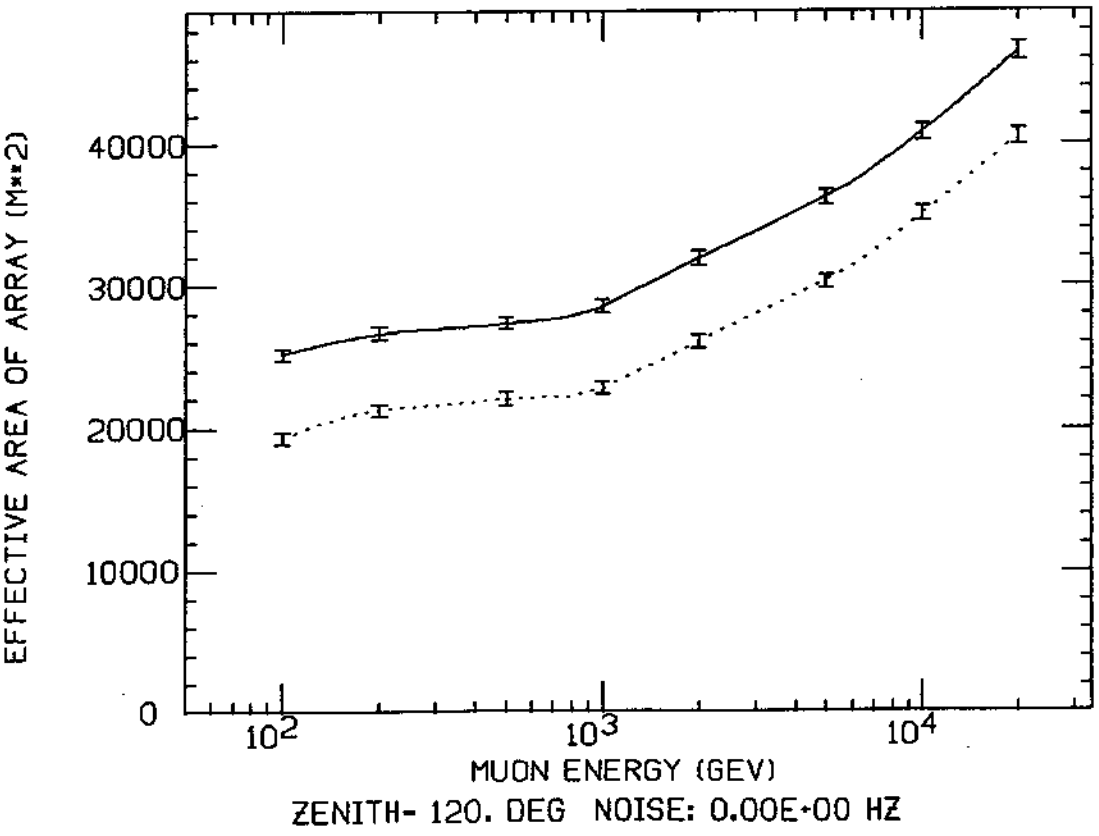
40000
30000
20000
10000
0
EFFECTIVE AREA OF ARRAY (M**2)
10^2
10^3
10^4
MUON ENERGY (GEV)
ZENITH- 120. DEG NOISE: 0.00E+00 HZ

Fig.3(b)

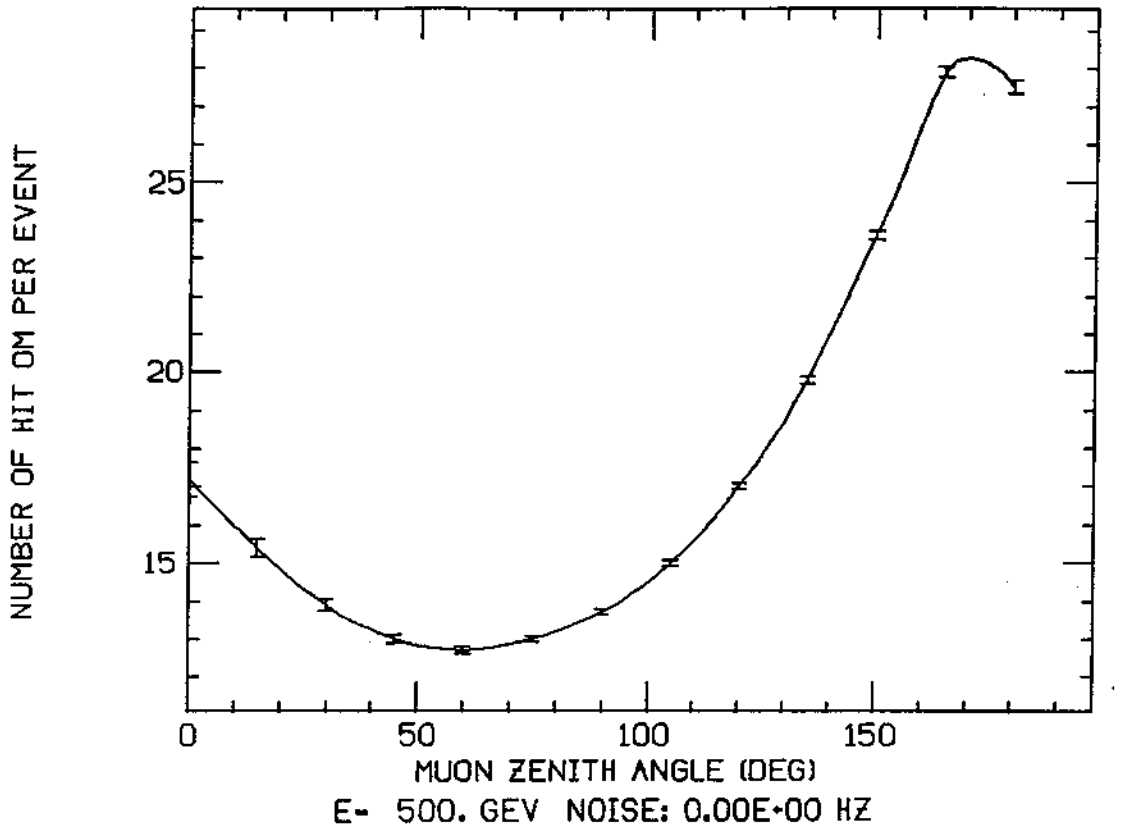
NUMBER OF HIT OM PER EVENT
25
20
15
0
50
100
150
MUON ZENITH ANGLE (DEG)
E- 500. GEV NOISE: 0.00E+00 HZ

Fig.4(a)

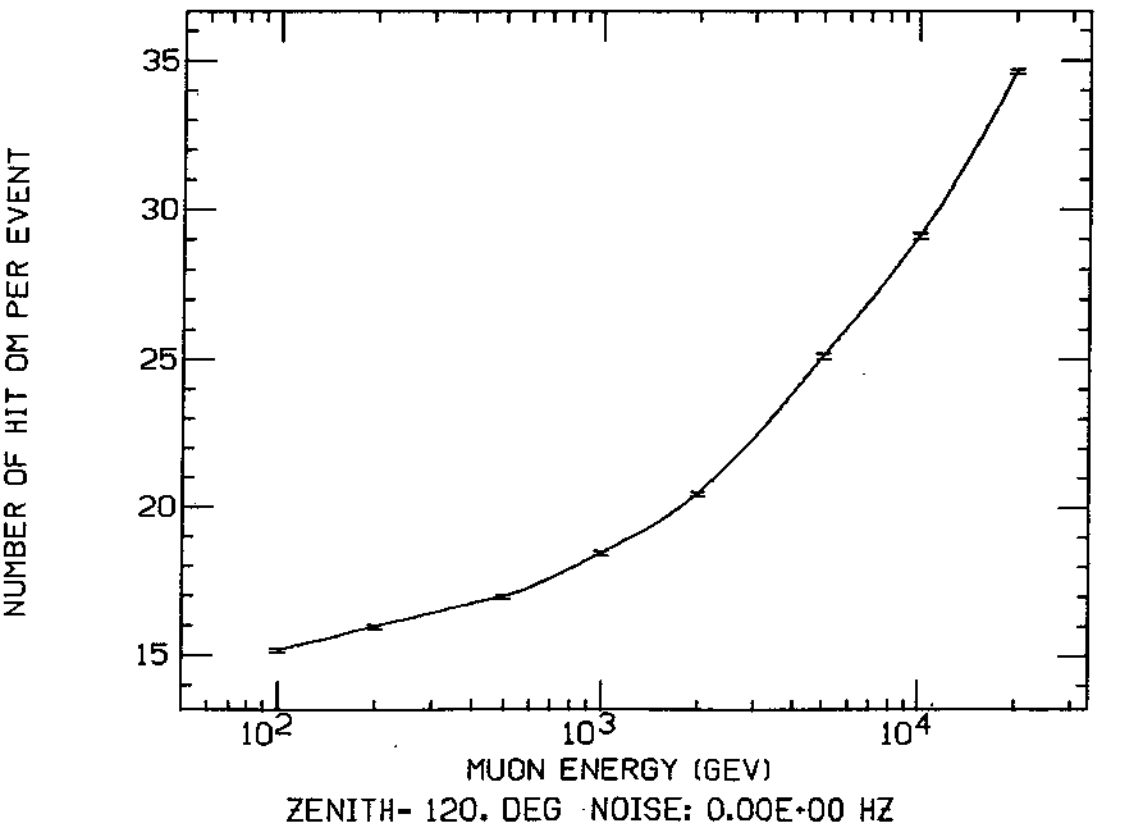
NUMBER OF HIT OM PER EVENT
35
30
25
20
15
10^2
10^3
10^4
MUON ENERGY (GEV)
ZENITH- 120. DEG NOISE: 0.00E+00 HZ

Fig.4(b)

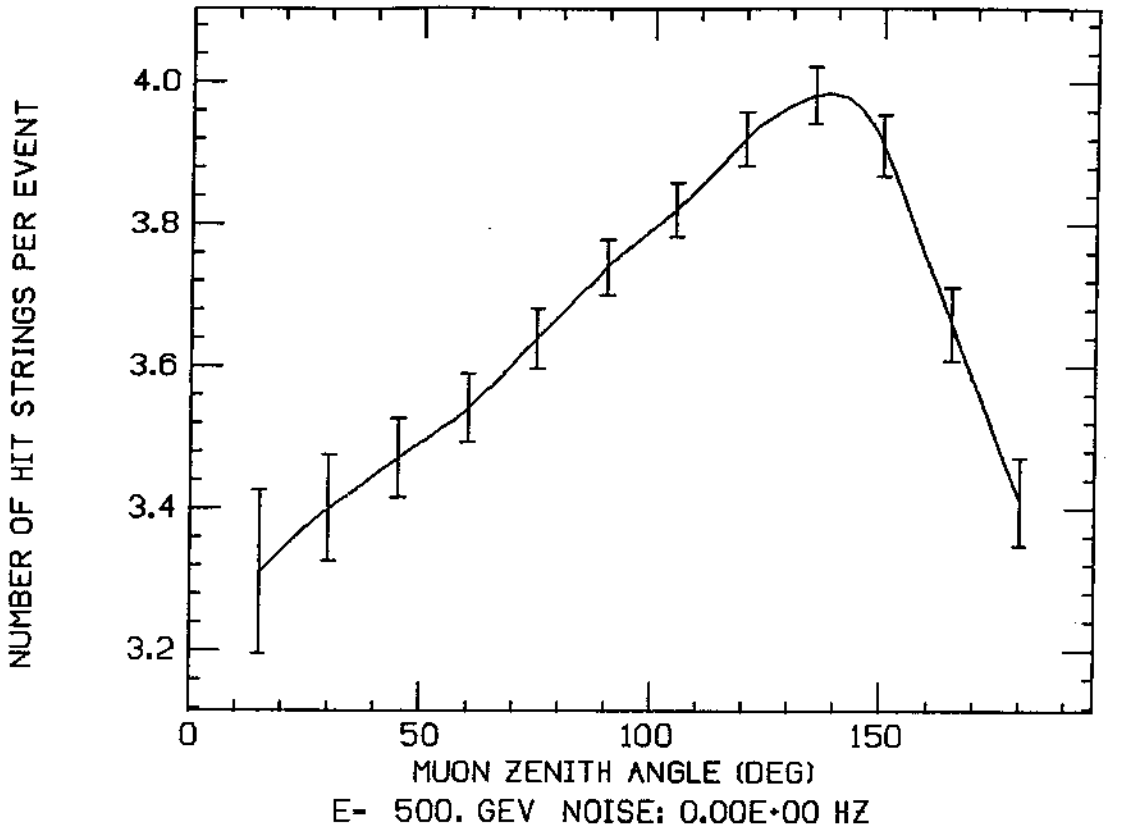
NUMBER OF HIT STRINGS PER EVENT
4.0
3.8
3.6
3.4
3.2
0
50
100
150
MUON ZENITH ANGLE (DEG)
E= 500. GEV NOISE: 0.00E+00 HZ

Fig.5(a)

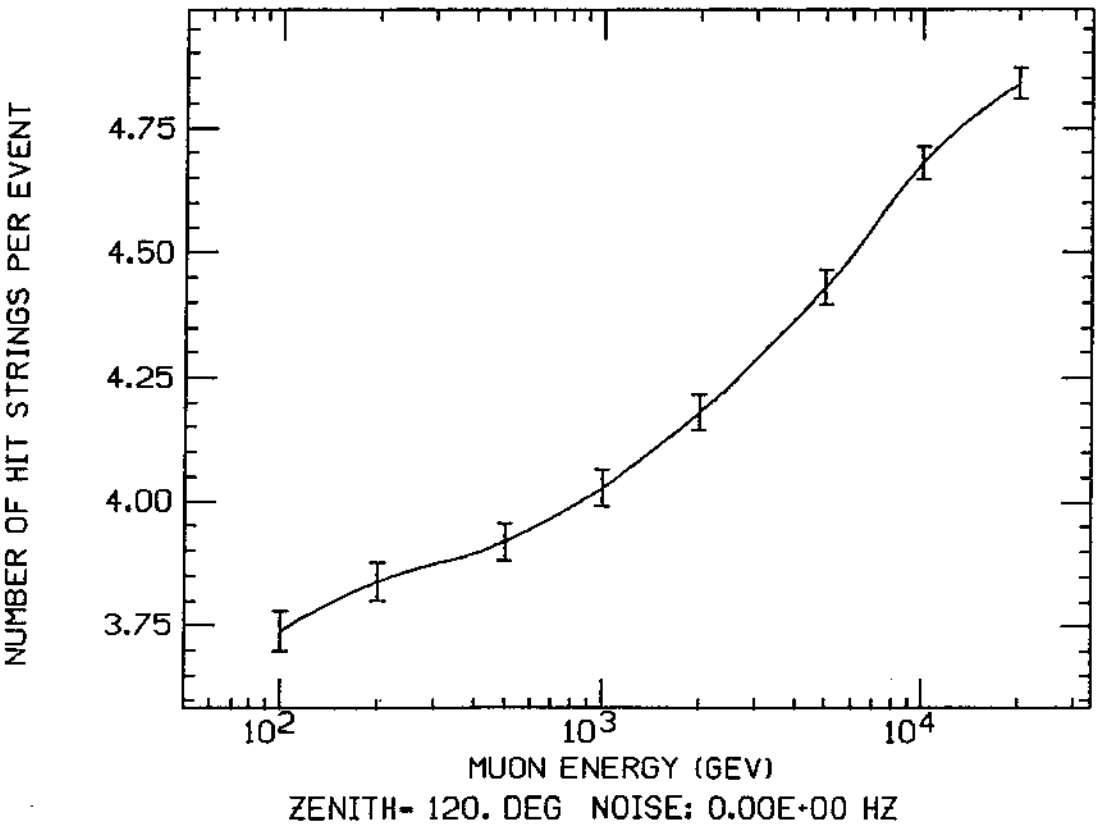
NUMBER OF HIT STRINGS PER EVENT
4.75
4.50
4.25
4.00
3.75
10^2
10^3
10^4
MUON ENERGY (GEV)
ZENITH= 120. DEG NOISE: 0.00E+00 HZ

Fig.5(b)

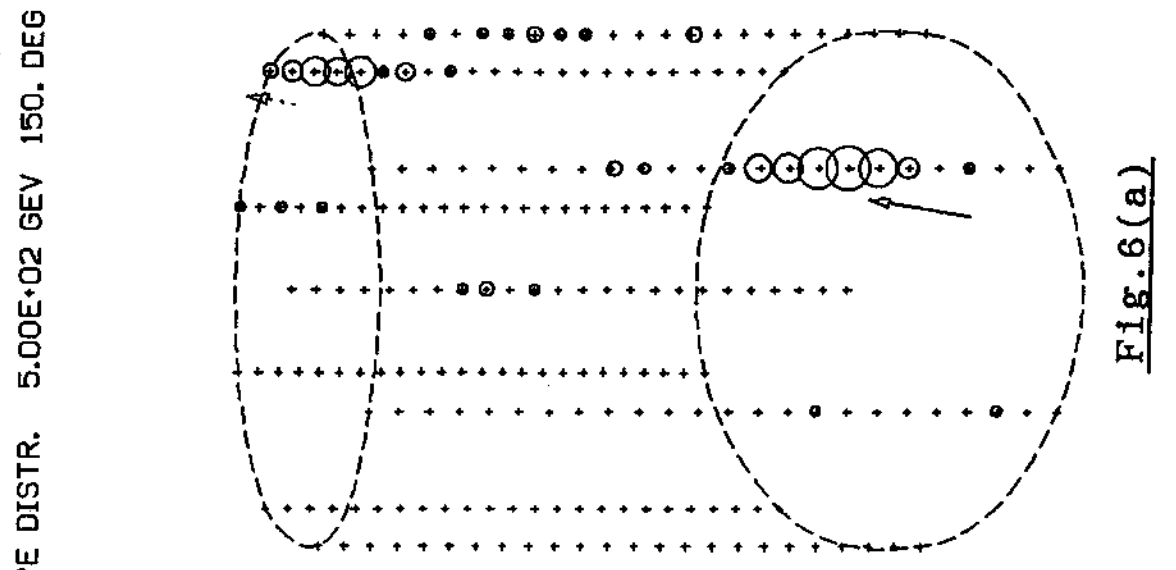

Fig.6(a)

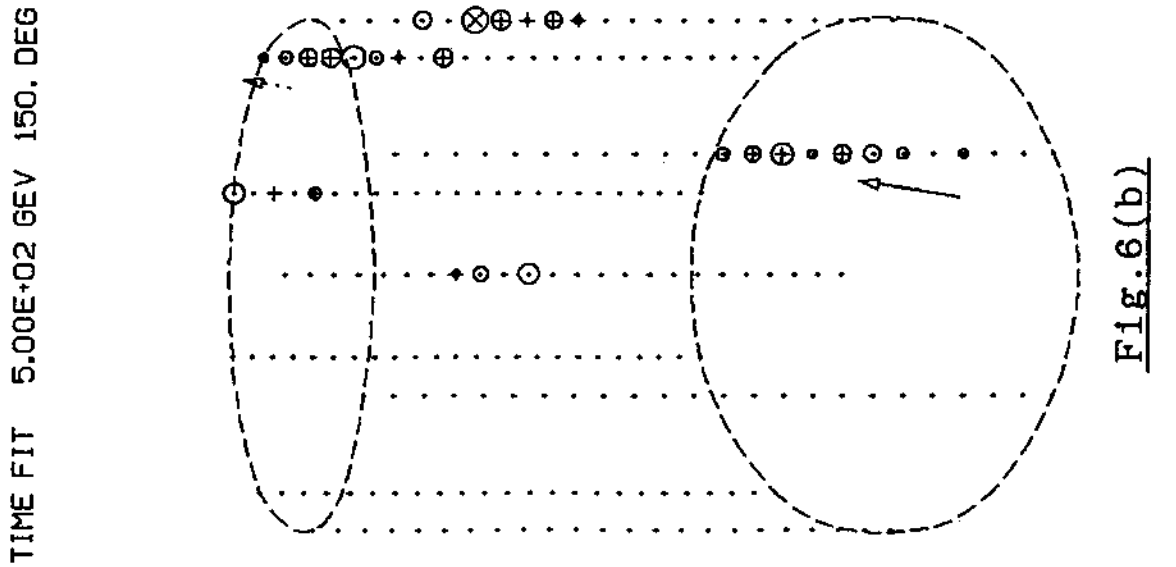

Fig.6(b)

ZENITH: 150. (ERROR: 0.1) CHI2/DF: 2.2E+00 (2.0E+00)
E-FACTOR: 0.37

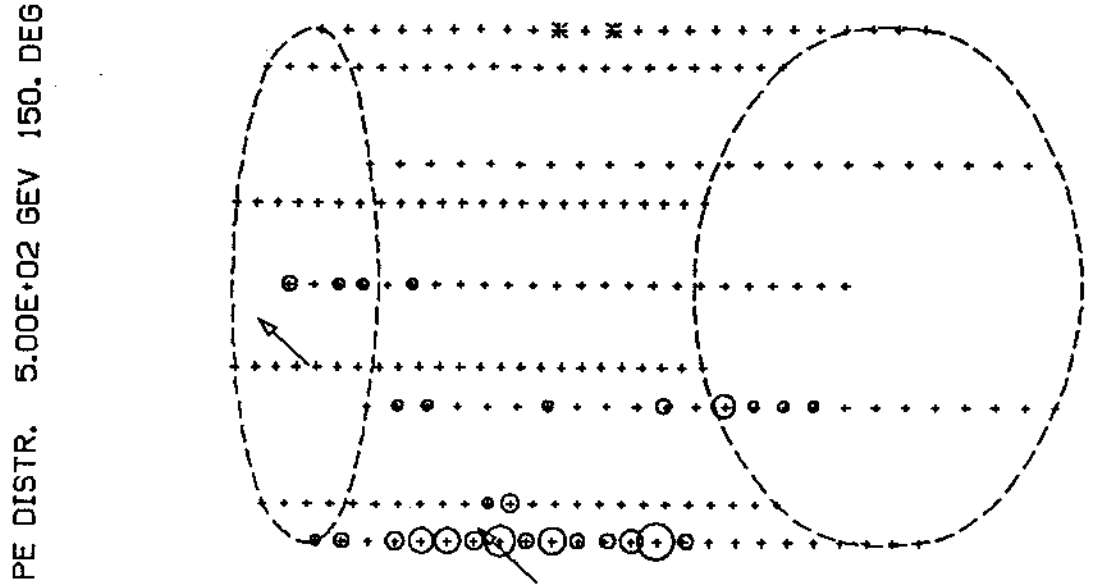

Fig.7(a)

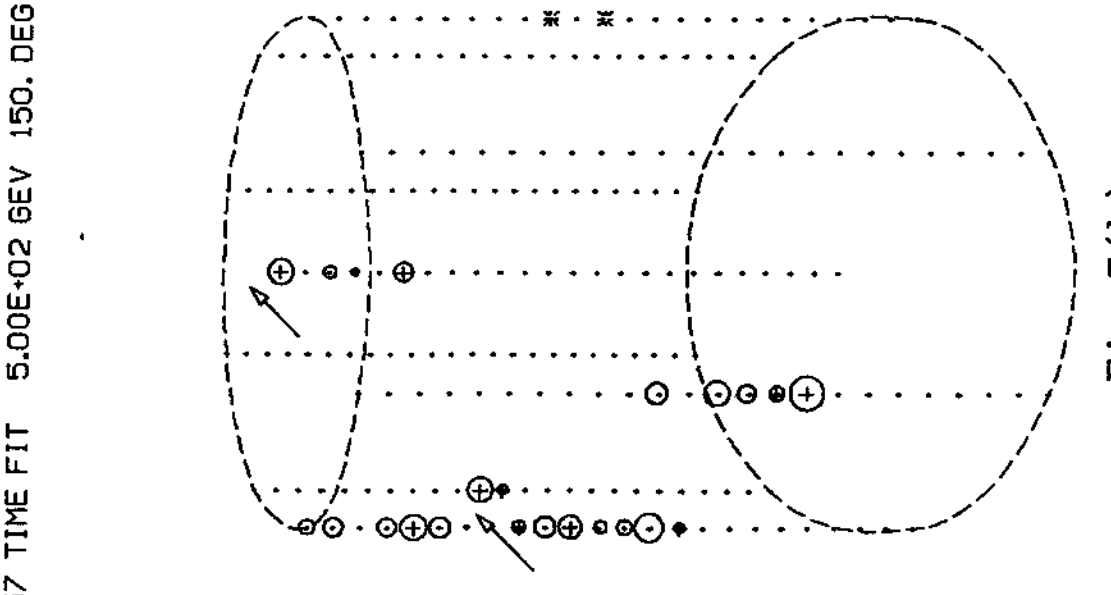

Fig.7(b)

ZENITH: 149. (ERROR: 1.6) CHI2/DF: 3.0E+00 (2.4E+00)
E-FACTOR: 0.42

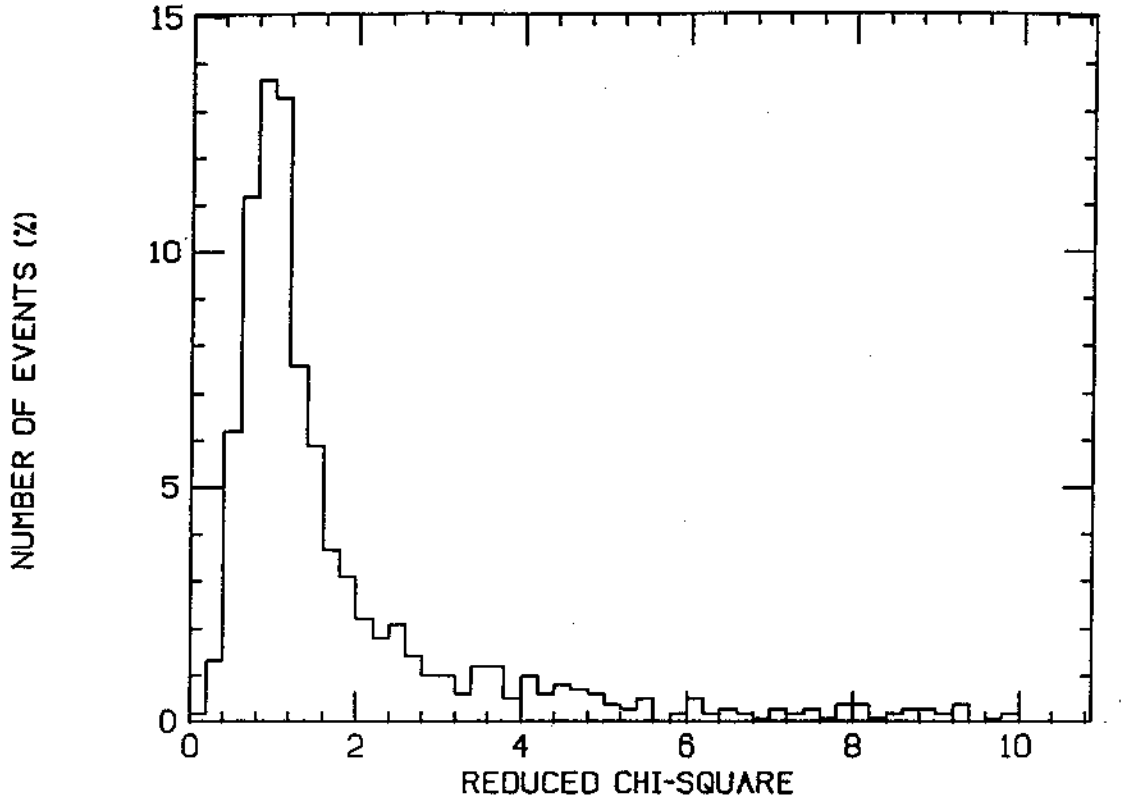

(ENTRY: 1628 TRIGGER: 1804/10000 MEDIAN: 1.31)
E- 500.GEV ZENITH- 120.DEG NOISE: 1.00E-05 HERZ

Fig.8

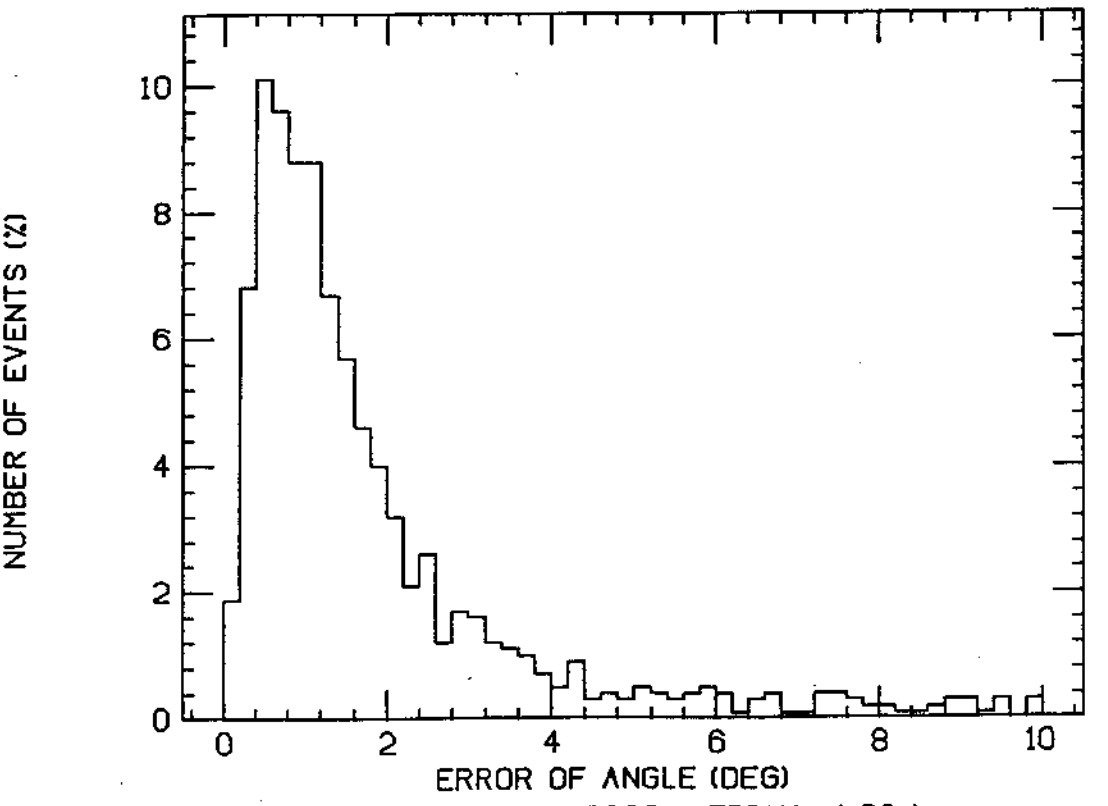

(ENTRY: 1139 OK: 1292/10000 MEDIAN: 1.32)
E- 500.GEV ZENITH- 120.DEG NOISE: 1.00E-05 HERZ

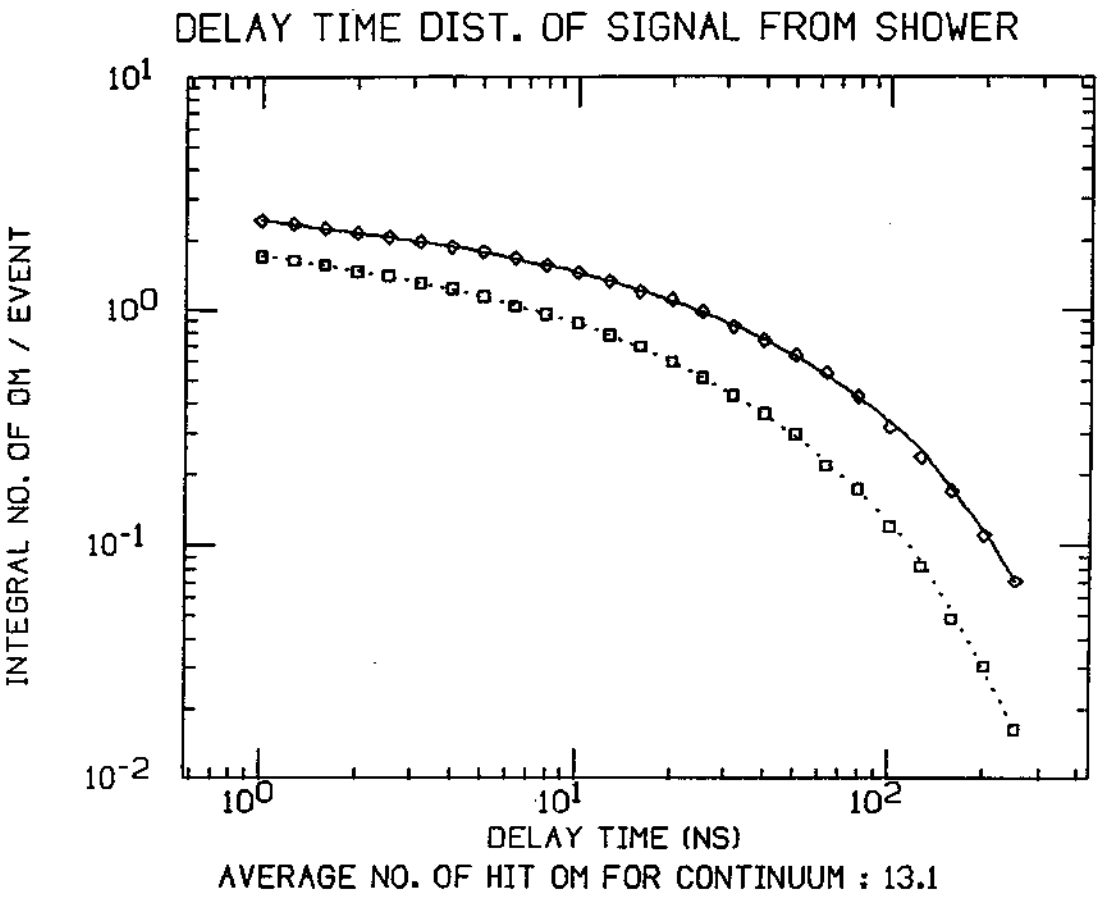
DELAY TIME DIST. OF SIGNAL FROM SHOWER
INTEGRAL NO. OF OM / EVENT
10^{1}
10^{0}
10^{-1}
10^{-2}
10^{0}
10^{1}
10^{2}
DELAY TIME (NS)
AVERAGE NO. OF HIT OM FOR CONTINUUM : 13.1

Fig.10